Catalysis Letters 14 (1992) 171–183

Influence of the preparation method on the characteristics of TiO_2-CeO_2 supports

A. Dauscher *, P. Wehrer and L. Hilaire

Laboratoire d'Etude de la Réactivité Catalytique, des Surfaces et Interfaces, URA 1498 du CNRS, Université Louis Pasteur, 4 rue Blaise Pascal, 67070 Strasbourg Cedex, France

Received 27 February 1992; accepted 10 April 1992

The preparation by a sol–gel process of TiO_2-CeO_2 supports (Ce/Ti atomic ratio = 1/1) was studied by varying the sol–gel processing conditions. Starting materials were $Ti[OCH(CH_3)_2]_4$ and $CeCl_3 \cdot 7H_2O$. The samples were characterised before and after calcination at 400°C by BET, porosity measurements, X-ray diffraction (XRD) and X-ray photoelectron spectroscopy (XPS). Working in acidic conditions leads to the formation of a compound that induces the growth of CeO_2 on amorphous TiO_2 during calcination. In a basic medium, a well defined $CeTiO_3$ compound is obtained that allows the formation of a real mixed TiO_2-CeO_2 compound after calcination. It presents a specific area of 70 $m^2\ g^{-1}$, a narrow distribution of mesopores and easily reducible cerium oxide.

Keywords: TiO_2; CeO_2; $CeTiO_3$; sol–gel process; XRD; XPS; BET

1. Introduction

The way of preparing TiO_2-SiO_2 oxides has become of great importance since they are used as supports of V_2O_5 for the selective catalytic reduction of NO with NH_3 [1–4]. Several methods have been reported such as the impregnation of a titanium chloride or alkoxide compound on SiO_2 [2,5,6] or the use of a sol–gel process with precipitation of the sols in the presence or absence of aqueous ammonia [1,3,7]. Different support characteristics were obtained by varying the sol–gel processing conditions [4]. In this paper, we deal with the preparation of TiO_2-CeO_2 mixed oxides supports by a sol–gel process. They present a remarkable stabilization of the +3 oxidation state of cerium if small amounts of CeO_2 are added to TiO_2 [8] and interesting yellow colouring properties [9–11]. Both the pH and the precipitation conditions are important factors leading to different specific areas, porosities and surface compositions.

* To whom correspondence should be addressed.

2. Experimental

2.1. PREPARATION OF THE SAMPLES

Starting solutions were prepared from tetraisopropylorthotitanate [$Ti(OCH(CH_3)_2)$] and $CeCl_3 \cdot 7H_2O$ as described in ref. [9]. The amounts used are such as to obtain Ce/Ti atomic ratios equal to 1. The common step of all the preparations is the dissolution at room temperature of 2 g of $CeCl_3 \cdot 7H_2O$ in 24 ml ethanol under magnetic agitation (pH = 4.0) and then the addition of 1.6 ml of the titanium alkoxide solution (pH = 1.5). As soon as the alkoxide is added, the solution becomes yellow, due to the combined action of a colour complex of cerium(IV)–titanium(IV) in the ratio 1/1 and to free Ce^{3+} ions [11]. No precipitation occurs. The pH conditions were then varied as well as the drying conditions:

Sample A: the solution is agitated during one hour and then let at room temperature. On the next day, it is gelled and some crystallisation appears. After 7 days, the gel is completely crystallised into bright yellow crystals of fleecy appearence.

Sample B: 0.5 ml H_2O are added to the solution, agitated during one hour, and let at room temperature. Next day, it is completely crystallised with the presence of two phases: a yellow one (diameter < 250 μm), similar to sample A, and an orange one constituted of aggregates that are very difficult to crush (diameter > 250 μm).

The direct addition of 2 ml H_2O leads to the complete hydrolysis of the sol and to the formation of the gel. If we let it crystallise, it becomes completely unhomogeneous (fine yellow crystals on large orange aggregates). If the gel is heated at 70°C, the result is the same. This method has not been retained.

Sample C: aqueous ammonia is added dropwise under agitation until the pH is equal to 9.0. When a drop of ammonia falls in the solution, a flocculent precipitate appears. When a basic pH is reached, a viscous brown-green gel is obtained that is destabilised in both a liquid and a solid phase when an excess of ammonia is added (pH = 9.0). The precipitate is filtered on a goosch filter, dried during 5 h and easily crushed.

Sample D is prepared like sample C but the precipitate is dried on a hot plate under agitation and the solvent is slowly evaporated. The formation of a white precipitate is observed on the cool walls of the beaker; it is eliminated as the deposit forms. The compound is less dense than sample C.

Sample E is prepared like sample C but the precipitate is dried in a rotatory evaporator.

Sample F is prepared like sample D but the precipitate is washed with water and dried. The operation is done 3 times.

Sample G is totally hydrolysed until we obtain a gel, before the addition of ammonia. The procedure follows then that of sample F. The obtained precipi-

tate is not homogeneous. It presents some dark grains more difficult to crush than the yellow-brown ones.

Sample H: H_2O is added until a yellow viscous gel is obtained. After addition of 2 ml CH_3COOH, the gel becomes an orange liquid. The solvent is evaporated on a hot plate. A viscous gel is formed again when the solvent is almost completely evaporated. The evaporation is pursued on the hot plate. No formation of orange aggregates is observed. The precipitate is crushed and washed twice with water. It is yellow and looks like sample A.

After the preparation, the samples are calcined under air at atmospheric pressure at 400°C in an oven. During calcination, water is released near 180°C and a white precipitate, smelling of ammonia, is formed at 380°C. A loss of roughly 40% in weight is observed for the samples prepared from ammonia. On sample D, the influence of the calcination temperature (from 400 to 900°C) with regard to BET and crystalline structure was studied.

The calcined samples will be named by their letter followed by the calcination temperature.

2.2. CHARACTERIZATION OF THE SAMPLES

BET specific areas were measured by N_2 physisorption at the temperature of liquid nitrogen. Pore size distributions were determined from the desorption isotherms of N_2 physisorbed at 77 K between the relative pressures $P/P_0 = 1$ and $P/P_0 = 0.3$, P_0 being the saturating vapour pressure. The numerical exploitations were done following Barett et al. [12]. X-ray diffraction (XRD) spectra were recorded using a Siemens D500 device.

X-ray photoelectron spectroscopy (XPS) analyses were performed on samples A400 and D400 without any further treatment. Sample D was studied like that, after evacuation at 200 and 400°C in situ in the preparation chamber of the XPS apparatus, and finally after calcination under air at 400 and 700°C, also in situ. The apparatus used is a VG ESCA III working with Al Kα as a photon source. The power on the anode was 120 W (12 kV $\times$ 10 mA). Relative surface compositions were calculated from photoelectron peak areas after correction for photo-ionization cross section [13] and difference in electron escape depth.

The interpretation of Ce 3d core level peaks is very difficult and since the first really well resolved spectra published fifteen years ago by Burroughs et al. [14], a lot of efforts have been devoted to their interpretation [15–19]. The assignment of the different structures is given in fig. 1a. Following Burroughs et al. [14], v, v″ and v‴ can be attributed to CeO_2; v and v″ are due to a mixture of $(5d6s)^0 4f^2$ $O2p^4$ and $(5s6d)^0 4f^1$ $O2p^5$ configurations while v‴ is a pure $(5d6s)^0 4f^0$ $O2p^6$ final state. On the other hand v_0 and v′ are due to a mixture of $(5d6s)^0 4f^2$ $O2p^4$ and $(5d6s)^0 4f^1$ $O2p^5$ configurations in Ce_2O_3. u structures, due to the Ce $3d_{3/2}$ level can be explained in the same way. Practically, a progressive reduction of Ce^{IV} into Ce^{III} will result in the decrease in $4f^0$ structures (v‴ and u‴),

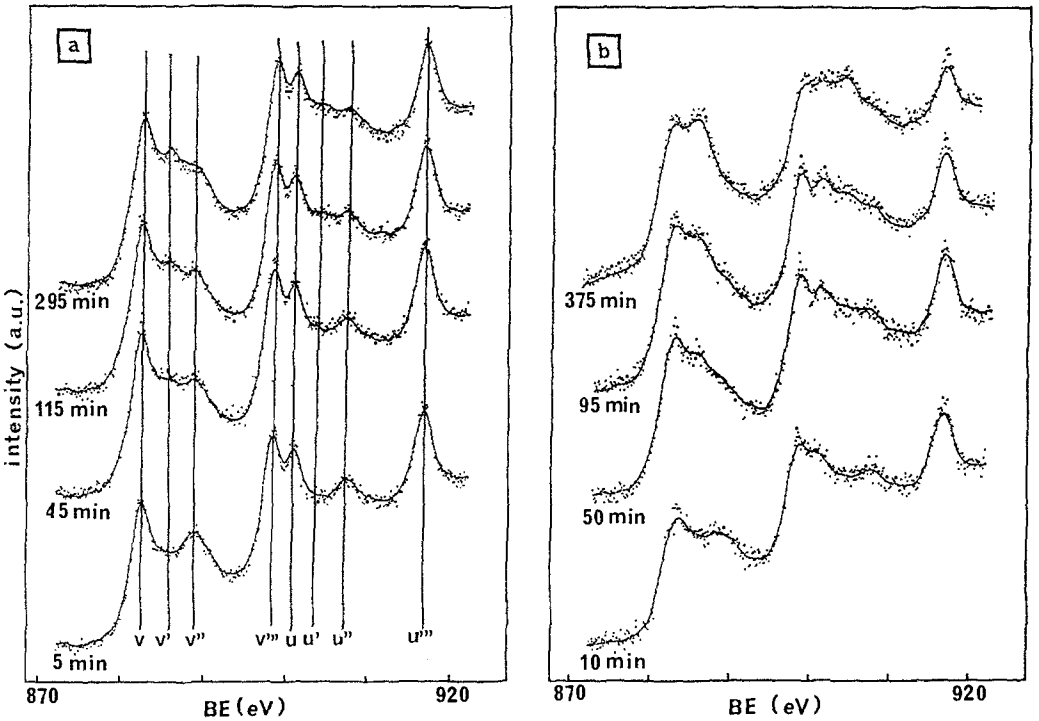

Fig. 1. XPS analyses of the Ce 3d core levels. Effect of the incident beam on the shape as a function of time. (a) Sample A400, (b) sample D400.

and in an increase in v′ and u′ at the expense of v″ and u″; v_0 and u_0 will be very difficult to resolve, at least for low degrees of reduction, because the energy separation with v and u is too small. We have developed in our laboratory a thorough analysis of Ce 3d XPS spectra allowing to give reliable quantitive data on the extent of reduction of CeO_2 under various conditions [20].

3. Results and discussion

Sample A presents a very low specific surface area (table 1) and XRD features that have not been identified (fig. 2a). No definite structure containing either titanium or cerium is detected. After calcination under air, the specific area is one order of magnitude higher. A mean pore size diameter of 7.6 nm is obtained (table 1) but the distribution of the pores is large (fig. 3), explaining the enhancement of specific area after calcination. The small pores are initially blocked by organic residues that are evacuated during calcination. The features of CeO_2 cerianite are then obtained (fig. 2b). No diffraction peaks corresponding to TiO_2, anatase or rutile, are detected. Moreover, the XPS results show

Table 1
Main characteristics of the various TiO_2-CeO_2 supports

Sample	Preparation	BET area ($m^2\ g^{-1}$)	Mean pore size diameter (nm)	Structure
A	drying at room temp.	6	–	?
A400		66	7.6	CeO_2, no TiO_2
B	H_2O, drying like A	–	–	–
B400		56	9.3	–
C	NH_3, filtration	2	–	$CeTiO_3$
C400		7.5	–	amorphous
D	NH_3, hot plate	74	15.8	$CeTiO_3$
D400		69	22.8	amorphous
E	NH_3, rotatory evaporator	–	–	–
E400		84	–	–
F	D, washing with H_2O	–	–	–
F400		46	–	–
G	H_2O, NH3, hot plate	–	–	–
G400		23	–	–
H	CH_3COOH, hot plate	–	–	–
H400		95	–	–

that only a little part of titanium is at the surface (Ce/Ti atomic ratio = 28 ± 2), while atomic absorption measurements show the expected 1/1 ratio (table 2). We have to postulate that the initially formed compound induces during calcination, first the growth of amorphous TiO_2 and then the growth of crystallised CeO_2 on that phase. Chlorine remains at the surface and in the bulk in the same proportions as shown by the Cl/Ce ratios obtained by the two characterization methods (table 2). Prolonged exposures to the X-ray beam in the XPS apparatus results in a reduction of cerium oxide as shown in fig. 1a. The v′ and u′ lines of the Ce 3d core levels, attributed to Ce^{III}, grow while the v″ and u″, attributed to Ce^{IV}, decrease. The amounts of Ce^{III} formed are enhanced from 10 to 20% during the first hour under the X-ray beam and are then stabilized to roughly 25% (fig. 4). Under the same experimental conditions, no variation of the oxidation state of cerium was observed for CeO_2 alone [21].

Adding water to accelerate the gelification leads to a small decrease in the specific area after calcination (sample B, table 1). Conversely, the presence of acetic acid lowers the gelification rate and induces an enhancement of the specific area (sample H, table 1). These results seem to show that the longer the gelification time is, the greater the specific area is.

The addition of aqueous ammonia leads to the precipitation of a well defined compound of $CeTiO_3$ composition (fig. 2c), whatever the drying procedure. The cerium orthotitanite has the perovskite structure with tetragonal symmetry [22]. No indexing of the diffraction pattern of $CeTiO_3$ is published though its crystallographic parameters have been defined [23,24]. Nevertheless the index-

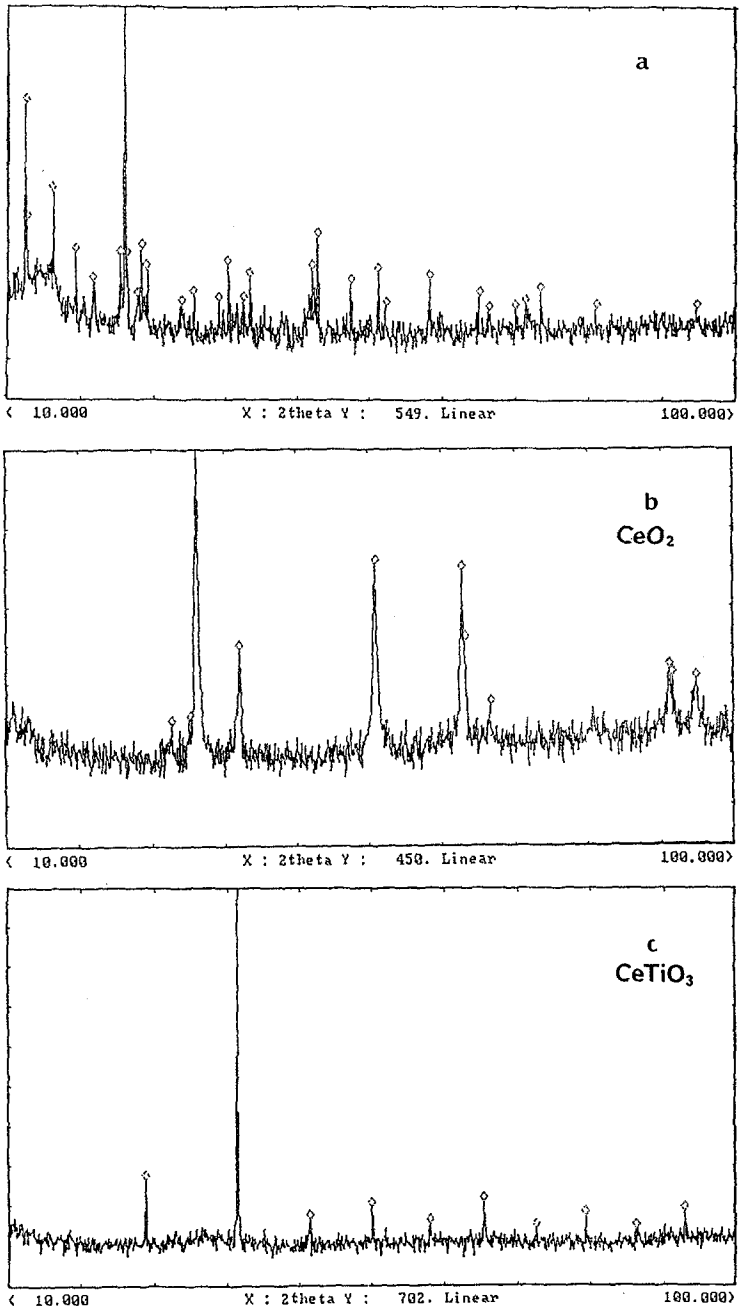

Fig. 2. XRD spectra. (a) Sample A (unidentified phases), (b) sample A400 (CeO_2), (c) sample D ($CeTiO_3$).

ing of $Ce_{2/3}TiO_3$ has been reported [25]. The spectra, as well as our crystallographic data fit very well with its indexing at the exception of a peak at 7.75 Å, characteristic of $Ce_{2/3}TiO_3$ and that does not exist in the spectra given for the

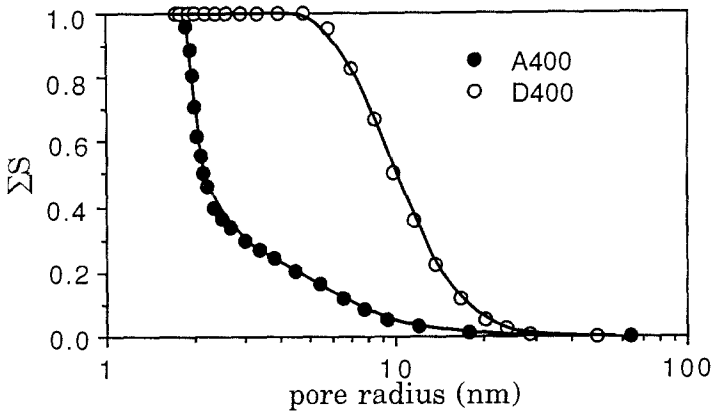

Fig. 3. Cumulative surface ΣS versus pore radius.

Table 2
Atomic ratios obtained by XPS and atomic absorption measurements on samples A400 and D400

Sample	XPS		Atomic absorption	
	Ce/Ti	Cl/Ce	Ce/Ti	Cl/Ce
A400	28	0.17	1.1	0.14
D400	1.1	0.21	0.9	0.25

$CeTiO_3$ compound itself. This fact allowed us to eliminate the possibility of a $Ce_{2/3}TiO_3$ formation and to assume the formation of $CeTiO_3$. In this compound, both Ce and Ti are in the +3 oxidation state, with a stoichiometric 1/1 ratio. The formation of this phase in very mild conditions, at room temperature, has never been reported. In the literature, it is prepared from mixtures of Ce_2O_3 and Ti_2O_3 sintered under vacuum at 1200°C during 50–60 h [23,24].

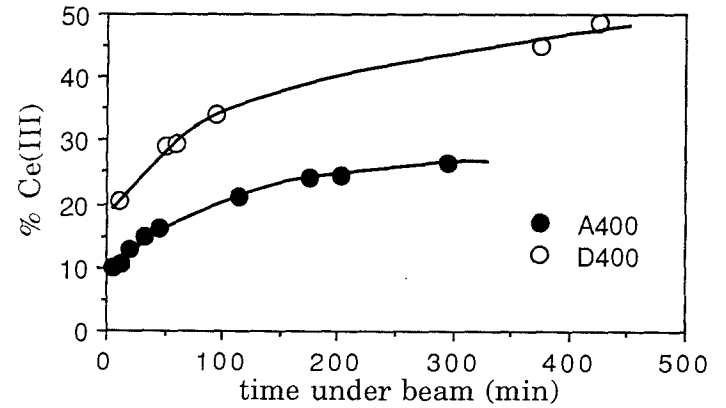

Fig. 4. Surface reduction of cerium during time under the X-ray beam in XPS analyses, for samples A400 and D400.

Table 3
Atomic ratios obtained by XPS on $CeTiO_3$

Treatment	Ce/Ti	Cl/Ce	C/Ti	N/Ti
without	1.1	2.5	2.8	1.2
evacuation 200°C	1.3	1.1	2.3	0.1
evacuation 400°C	1.3	1.6	2.2	0
air 400°C	0.9	0.4	0.9	0
air 700°C	0.8	0.05	0.9	0

Nevertheless, the presence of many impurities remaining at the surface and in the bulk is obvious. No definite other phase such as CeOCl is, however, obtained.

In order to clean $CeTiO_3$, it was treated at atmospheric pressure under flows of Ar at 200, 400, 600 or 800°C. The treatments lead to the disappearance of the $CeTiO_3$ features above 200°C. The obtained compound is amorphous to X-rays after calcination at 200 or 400°C and new features appear at 600 and 800°C, that are not TiO_2 or CeO_2. The features do not correspond to any known definite compound.

XPS analyses confirm that in the initial compound, the amounts of impurities (Cl, C and N) are high (table 3). Nitrogen is easily removed by evacuation. Chlorine is partly removed by evacuation but disappears almost totally after the treatments under air. Carbon is not at all eliminated by evacuation and it is only partly removed from the surface after the air treatments, even after 700°C. The Ce/Ti atomic ratios have nearly the expected value of 1. They are a little higher when the amounts of chlorine at the surface are high, perhaps due to the affinity of cerium towards chlorine. In fig. 5 are reported the spectra of the Ce 3d levels after various treatments. The spectra were recorded 5 min after switching on the anode. In the initial $CeTiO_3$ compound (fig. 5a), cerium oxide is less reduced than after evacuation at 400°C (fig. 5c) where roughly 70% of Ce^{III} is detected. So, evacuation at 400°C does not, a priori, destroy the structure. Moreover, in that case, a quantity of roughly 8% of Ti^{III} is found (fig. 6), confirming that at least a part of the compound has the $CeTiO_3$ structure, even at the surface. Treatments under air lead to the total decomposition of $CeTiO_3$ into CeO_2 (figs. 5d and 5e).

After calcination under air at 400°C, the oxidation products are amorphous to X-rays. When the calcination temperature is enhanced, a change in the colour of the compound is observed between 600 and 700°C, from mustard yellow to pale yellow. The features of CeO_2 cerianite become apparent from 600°C and the peak intensities increase with the calcination temperature. The TiO_2 rutile phase was not observed before 900°C and even at this temperature it was poorly crystallised. There is also the very diffuse presence of a non-established phase that may be $CeTi_2O_6$. These results agree with the ones obtained by Bazuev et

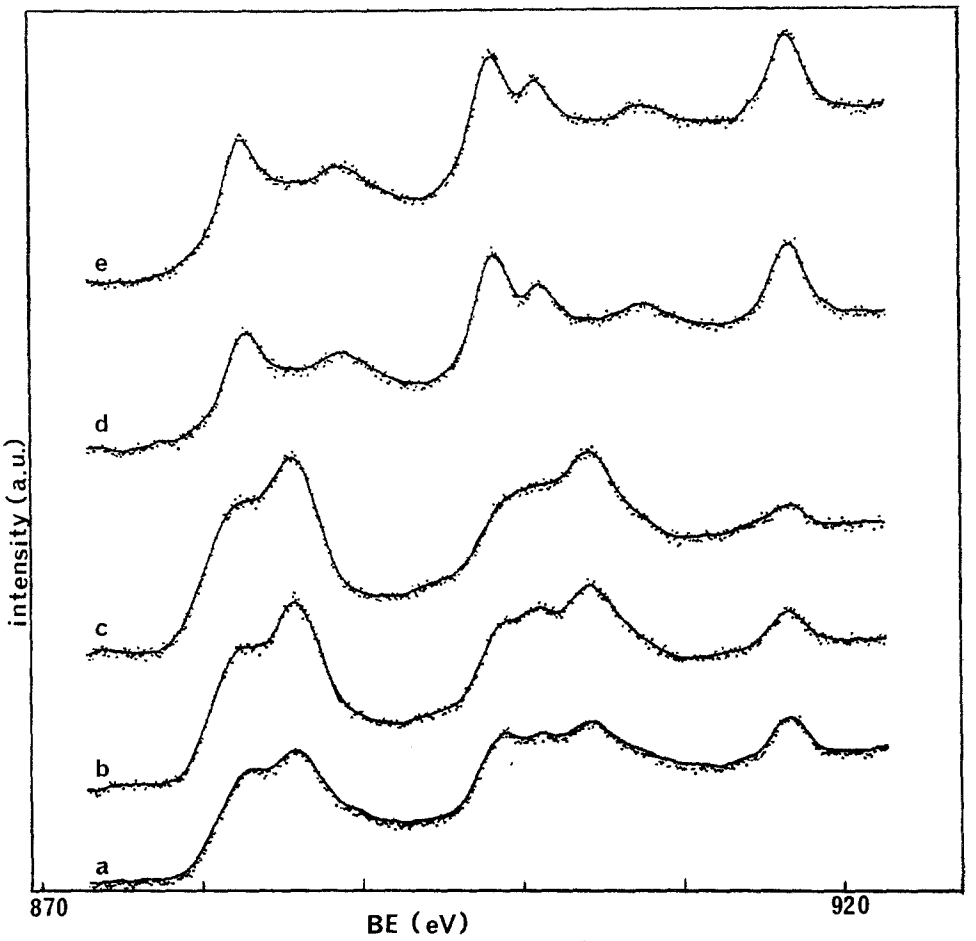

Fig. 5. Ce 3d spectra of $CeTiO_3$. (a) Without any treatment, (b) after evacuation at 200°C, (c) after evacuation at 400°C, (d) after air treatment at 400°C and (e) after air treatment at 700°C.

al. [23]. They have isolated a new green intermediate poorly crystallising phase after heating in air at 450–500°C for 6–8 h, from approximate composition $CeO_2 \cdot TiO_2$. Nevertheless, it was not possible for them to draw a definite conclusion about the formation of the compounds $CeTi_2O_{5.6}$ and $CeTi_3O_{8.7}$ as intermediate oxidation products.

The specific area varies with the way of drying the cerium orthotitanite (table 1). A simple filtration of the product leads to the poorest surface even after calcination (sample C). The evaporation of the solvent on a hot plate, near 70°C, leads to a surface of roughly 70 $m^2\ g^{-1}$ both with or without calcination (sample D) whereas the mean pore size diameter is enhanced to 22.8 nm, with a very narrow distribution of mesopores (fig. 3b). The calcination treatment must induce both the sintering of the small pores (enhancement of the mean pore size diameter) and the release of impurities such as water, chloride or ammonia compounds from the mesopores (no decrease of surface though sintering occurs).

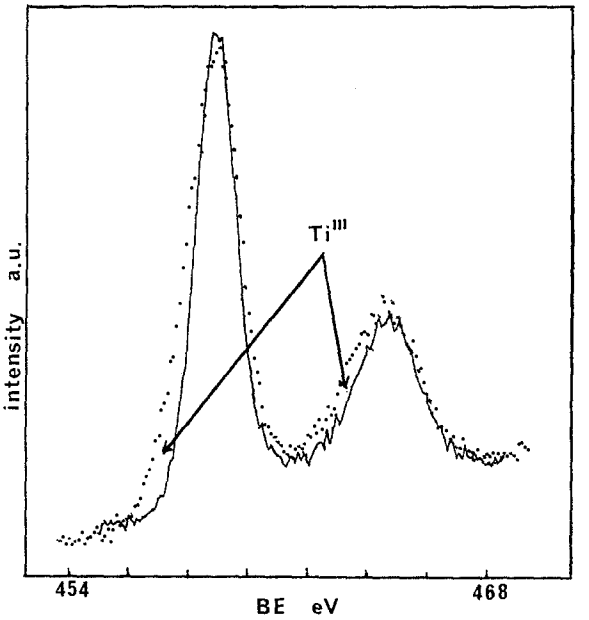

Fig. 6. Ti 2p spectra of $CeTiO_3$ (full line: without any treatment, dotted line: after evacuation at 400°C).

The use of a rotatory evaporator leads to a slightly higher surface (sample E), while fast gelification, due to the addition of water, induces a loss of surface (sample G). Therefore, like for the first type of samples (A, B, H), the ageing of the gel has an influence on the specific area obtained: the more the gel is aged, the greater the surface is.

Washing the sample with water leads to a great decrease of the surface (sample F). It must be due to the presence of some water remaining at the surface that induces an easier sintering of the pores during calcination.

The increase in the calcination temperature, studied with sample D, leads to a linear decrease of the surface, of 11 ± 2 m^2 g^{-1} per 100°C (fig. 7), showing that it easily sinters, i.e. it is not very resistant to high temperature under air.

XPS results obtained on sample D400 show that the atomic surface Ce/Ti ratio is equal to the expected value of 1.0 ± 0.1, contrarily to sample A400 (table 2). This value is in agreement with the value obtained by bulk analyses. It is interesting to note that this ratio is obtained even after calcination. We can believe that the initial $CeTiO_3$ compound has induced the formation of a real mixed TiO_2-CeO_2 oxide, even if it is amorphous to X-rays, with a close contact between titanium and cerium atoms. This would be a good method for the preparation of the TiO_2-CeO_2 supports.

Like for sample A400, little amounts of chlorine are retained at the surface and in the bulk. This means that the calcination temperature is not high enough to completely eliminate chlorine.

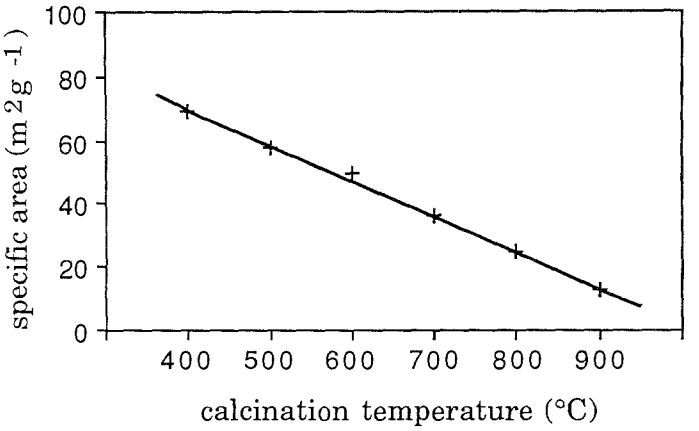

Fig. 7. Variation of the BET area of sample D as a function of calcination temperature.

The modifications of the Ce 3d core level spectra as a function of time of exposure under the X-ray beam are more important than for sample A400 (fig. 1b). The percentage of Ce^{III} varies from 20 to 50% under the beam in 400 min (fig. 4). The line shape of the curve indicates that it is still not stabilised at this value. These experiments, with samples A400 and D400, clearly show the importance of the close presence of titanium on the reduction phenomena of cerium. Moreover, a narrowing of 0.2 eV of the Ti 2p core level peaks is observed during time under the beam (fig. 8). This suggests that the electron density of titanium may be lowered and could explain, but only partly, the reduction of cerium oxide. The modifications of the titanium core level peaks under the beam have to be confirmed by using a monochromatic X-ray source, in order to see the very fine variations of the shape of the peaks.

Finally, the supports that will be used in catalysis will be prepared like sample D because they present relatively high specific areas, a narrow distribution in mesopores and a close neighbourhood of titanium and cerium atoms allowing the easy reduction of cerium. The latter fact can be useful in reactions like the selective hydrogenation of α, β-unsaturated aldehydes that we have already begun to study.

4. Conclusion

The change of the pH conditions allowed us to prepare two series of TiO_2-CeO_2 supports. In an acidic medium, the formation of some unidentified crystallising phases of low specific area are observed. Calcination induces the covering of amophous TiO_2 by crystallised CeO_2. In a basic medium, a well defined $CeTiO_3$ compound is obtained. The preparation of this compound in very mild conditions has never been reported. Nevertheless, the stucture is not

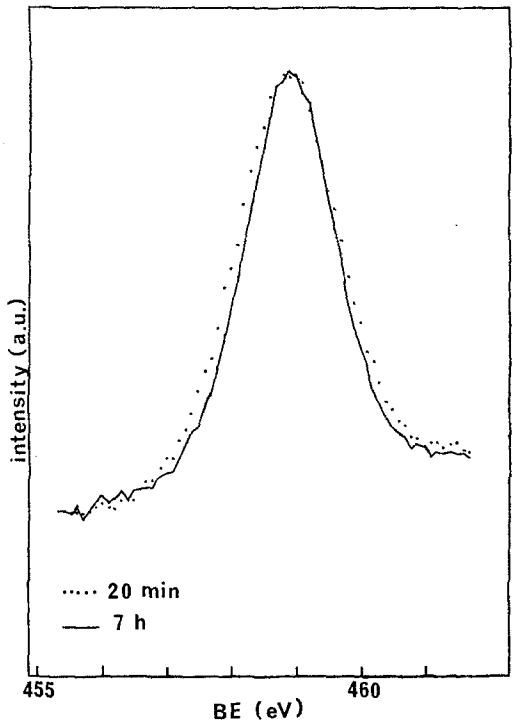

Fig. 8. XPS spectra of the Ti 2p core levels on sample D400 20 min (dots) and 7 h (full line) after switching on the photon source, respectively.

kept by heating. After calcination, it becomes amorphous but the 1/1 stoichiometry is kept. XPS analyses allowed us to see that cerium is no longer in the +3 oxidation state. Nevertheless, the close neighbourhood of titanium atoms induces an easy reduction of cerium oxide. The so-prepared TiO_2-CeO_2 supports have a high specific area and a narrow distribution of mesopores. In both series, ageing of the gels leads to higher specific areas.

Acknowledgement

The authors thank Dr. C. Petit for helpful discussions.

References

[1] A. Baiker, P. Dollenmeir and M. Glinski, Appl. Catal. 35 (1987) 365.
[2] R.A. Rajadhyaksha, G. Hausinger, H. Zeilinger, A. Ramstetter, H. Schmelz and H. Knözinger, Appl. Catal. 51 (1989) 67.
[3] K.L. Walther, M. Schraml-Marth, A. Wokaun and A. Baiker, Catal. Lett. 4 (1990) 327.
[4] B.E. Handy, A. Baiker, M. Schraml-Marth and A. Wokaun, J. Catal. 133 (1992) 1.

[5] A. Fernandez, J. Leyrer, A.R. Gonzalez-Elipe, G. Munuera and H. Knözinger, J. Catal. 112 (1988) 489.
[6] M.A. Reichmann and A.T. Bell, Langmuir 3 (1987) 111.
[7] M. Itoh, H. Hattori and K. Tanabe, J. Catal. 35 (1974) 225.
[8] A. Dauscher, L. Hilaire, F. Le Normand, W. Müller, G. Maire and A. Vasquez, Surf. Inter. Anal. 16 (1990) 341.
[9] A. Makishima, H. Kubo, K. Wada, Y. Kitami and T. Shimohira, J. Am. Ceram. Soc. 69 (1986) C-127.
[10] A. Makishima, M. Asami and K. Wada, J. Non-Cryst. Solids 121 (1990) 310.
[11] M.A. Sainz, A. Duran and J.M. Fernandez Navarro, J. Non-Cryst. Solids 121 (1990) 315.
[12] E.P. Barrett, I.G. Joyner and P.P. Halenda, J. Am. Chem. Soc. 73 (1951) 373.
[13] J.H. Scofield, J. Electron Spectry. Relat. Phen. 8 (1976) 129.
[14] P. Burroughs, A. Hammett, A.F. Orchard and G.J. Thornton, Chem. Soc. Dalton Trans. (1976) 1686.
[15] A. Fujimori, Phys. Rev. B28 (1983) 4489.
[16] A. Kotani, H. Mizuta, J. Jo and J.C. Parlebas, Solid State Commun. 53 (1985) 805.
[17] A. Nakano, A. Kotani and J.C. Parlebas, J. Phys. Soc. Japan 56 (1987) 2201.
[18] A. Kotani and J.C. Parlebas, Adv. Phys. 37 (1988) 37.
[19] F. Le Normand, J. El Fallah, L. Hilaire, P. Légaré, A. Kotani and J.C. Parlebas, Solid State Commun. 71 (1989) 885.
[20] M. Romeo, K. Bak, J. El Fallah, F. Le Normand and L. Hilaire, J. Phys. Chem., submitted.
[21] J. El Fallah, PhD Thesis, Université Louis Pasteur, Strasbourg (1992).
[22] G.V. Bazuev and G.P. Shveikin, Russ. J. Inorg. Chem. 22 (1977) 675.
[23] G.V. Bazuev, O.V. Makarova, V.A. Zhiluaev and G.P. Shveikin, Russ. J. Inorg. Chem 21 (1976) 1447.
[24] V.H. Holzapfel and J. Sieler, Z. Anorg. Allg. Chem. 343 (1966) 174.
[25] G.V. Bazuev, O.V. Makarova and G.P. Shveikin, Russ. J. Inorg. Chem. 23 (1978) 800.